analytical chemistry

Technical Note

pubs.acs.org/ac

Reducing pH Gradients in Free-Flow Electrophoresis

Fletcher J. Agostino, Leonid T. Cherney, Mirzo Kanoatov, and Sergey N. Krylov*

York University, Department of Chemistry and the Centre for Research on Biomolecular Interactions, 4700 Keele St., Toronto, Ontario M3J 1P3, Canada

Supporting Information

ABSTRACT: Small-volume continuous-flow synthesis (small-volume CFS) offers a number of benefits for use in small-scale chemical production and exploratory chemistry. Typically, small-volume CFS is followed by discontinuous purification; however, a fully continuous synthesis-purification combination is more attractive. Milli free-flow electrophoresis (mFFE) is a promising continuous-flow purification technique that is well suited for integration with small-volume CFS. The purification stability of mFFE, however, needs to be significantly improved before it can be feasible for this combination. One of the major sources of instability of mFFE is attributed to the ions produced as a result of electrolysis. These ions can form pH and conductivity gradients in mFFE, which are detrimental to separation quality. The severity of these gradients has not been thoroughly studied in mFFE. In this paper, we have experimentally demonstrated that detrimental pH gradients occur at flow rates of 8 mL/min and less, and electric field strengths of 25 V/cm and greater. To decrease the pH gradients, it is necessary to evacuate H^+ and OH^- as soon as they are generated; this can be done by increasing local hydrodynamic flow rates. We calculated the necessary flow rate, to be applied at the electrode, which can effectively wash away both ions before they can cause a detrimental pH gradient. These optimized flow rates can be attained by designing a device that incorporates deep channels. We have confirmed the effectiveness of these channels using a prototyped device. The new design allows mFFE users to work over a wider range of flow-rate and electric-field conditions without experiencing significant changes in pH.

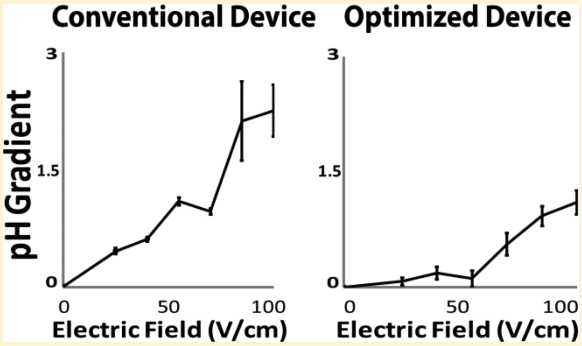

Chemical synthesis can be carried out in either a discontinuous (batch) or continuous-flow manner. Historically, continuous-flow synthesis (CFS) has predominantly existed in large-scale industrial settings for the purpose of process streamlining.[1] However, it is becoming evident that CFS has additional advantages that make it attractive for use in small-scale production and exploratory chemistry (small-volume CFS). These advantages include increased precision when controlling reaction conditions (i.e., mixing, temperature, pressure),[2,3] the possibility of performing high temperature and high pressure reactions,[4] easy scaling-up techniques for larger product quantities,[5,6] safer handling of hazardous reactions,[7] in-line monitoring of products,[8] and automation capabilities.[9,10] Recently, generic equipment for small-volume CFS has been made commercially available and has been used for a variety of chemical reactions.[11−13]

Typically, CFS is followed by discontinuous purification. It is desirable to combine CFS with continuous-flow purification (CFP) in order to take advantage of its automation capacity and real-time feedback and control.[10] However, implementing a completely continuous process remains challenging, because of a limited number of suitable CFP techniques.[14] Free-flow electrophoresis (FFE) has been suggested as an attractive method for total continuous processing.[15] The purification stability of FFE, however, needs to be significantly improved before it can be used for this purpose.

In FFE, samples are carried through a wide separation channel by a buffer flow and resolved into their individual components by an electric field applied in the direction orthogonal to the flow.[16,17] FFE instability arguably stems from electrolysis, which accompanies the application of an electric field. The quality of FFE purification deteriorates within minutes due to the production of both gas bubbles (H_2 and O_2) and ions (H^+ and OH^-) at the electrodes. The bubble problem has been studied thoroughly[18−21] and ultimately resolved by the introduction of open-electrolyte FFE (OEFFE).[22] The ion problem, however, has not been comprehensively studied.

The electrolytic ions, H^+ and OH^-, pose a problem because of their migration from the electrodes into the separation channel, where they can potentially alter the pH and conductivity of the electrolyte. Such pH gradients are undesirable when analyzing pH-sensitive species. pH gradients can affect the analytes by altering their structural conformation, reactivity, and optical properties (which can render the analytes undetectable). In addition, the establishment of pH and conductivity gradients may diminish FFE separation quality by altering sample stream trajectories and causing band broadening.[23] In the macro-FFE format (mL to L/min flow

Received: March 25, 2014
Accepted: May 16, 2014
Published: May 16, 2014

   dx.doi.org/10.1021/ac501081b | Anal. Chem. 2014, 86, 5656−5660

rates), the adverse effects of pH gradients on separation efficiency have been observed, studied, and alleviated by introduction of ion-impermeable membranes.[24] The use of membranes, however, always reduced the effective electric field strengths in FFE experiments and, thus, decreased their electrophoretic resolution efficiency.[25−27] The pH gradients in the micro-FFE format (nL to μL/min flow rates) have only been studied in the context of ampholyte distribution in isoelectric focusing.[28] Furthermore, both the macro- and micro-FFE formats operate at flow rates that are difficult to adapt to small-volume CFS. Our previous studies suggest that flow rates used in small-volume CFS are best-matched with the milli-FFE format (mFFE) which operates with a μL to mL/min flow rate range.[29] To date, pH gradients in mFFE have not been studied.

In this work, we have experimentally demonstrated that pH gradients do occur in mFFE devices. These results defined a set of conditions at which pH gradients become significant. We hypothesized that the ions can be rapidly and effectively washed away, at the electrode, before causing pH gradients. We optimized the geometry of channels within the mFFE device to attain the necessary flow rates. We also investigated any influence that these channels might have on the hydrodynamic flow by modeling the flow profiles in a virtual device. Lastly, we confirmed the effectiveness of the virtual solution with a prototyped device.

EXPERIMENTAL SECTION

Chemicals and Reagents. All reagents were purchased from Sigma-Aldrich, unless otherwise stated. A 25 mM 4-(2-hydroxyethyl)-1-piperazine-ethanesulfonic acid (HEPES, 99.5% purity) buffer solution with Triton X-100 (0.001% [w/v]) was adjusted to pH 7 with 10 M NaOH and used in all experiments. The buffer mixture was deoxygenated by overnight N_2 bubbling. A separate 10% EtOH solution was used as a primary wash solution to wet the surfaces of the mFFE devices. All solutions were prepared using deionized H_2O (EMD Millipore, Mississauga, Canada), the electrical resistivity of which was 18.2 MΩ·cm. The hydrodynamic flow of the buffer was driven by a continuous flow syringe pump system (New Era Pump System Inc., Farmingdale, NY, USA). The power source used was a high-voltage Electrophoresis Power Supply EPS 3501 XL (Amersham Pharmacia Biotech, New Jersey, USA).

mFFE Device Operation. The fabrication of mFFE devices is described in the Supporting Information. The buffer flow rates ranged from 1.00 ± 0.05 to 8.00 ± 0.05 mL/min. The electric field strengths used ranged from 25 to 100 V/cm inside the separation channel. Experiments were carried out at room temperature. The mFFE devices were placed on top of metal blocks, which were in contact with ice packs, to prevent overheating. Buffer elution fractions were collected from two outlets, and their pH was measured using the Orion benchtop pH/mV/temperature/ion meter model 710A (ThermoFisher Scientific, Waltham, MA, USA).

COMSOL Simulations. To simulate and study flow profiles in mFFE devices, we used COMSOL Multiphysics software version 4.3b. A virtual 3D model of the separation channel was created using discrete geometry. The 3D results are illustrated in a 2D format for ease of visualizing the flow profiles. A steady state virtual system was designed using the Laminar Flow module. Conditions and settings for the simulations have been described previously.[22] The setup and comprehensive theory and equations, associated with all COMSOL simulations, can be found in the Supporting Information.

RESULTS AND DISCUSSION

Our mFFE device (Figure 1) consists of a wide separation channel (SC) with wire electrodes on opposite sides that span its entire length. The buffer enters the SC as a uniform hydrodynamic flow and carries a sample mixture, which is introduced downstream of the buffer entry. As a sample mixture travels through the applied electric field, it is resolved into individual component streams, which are defined by their respective electrophoretic mobilites. Electrophoretic conditions are chosen to maximize the separation between component streams and to direct them toward a row of collection outlets. The distance between the terminal outlets, anode outlet (AO) and cathode outlet (CO), is defined as the separation zone (SZ). The space between each of the terminal outlets and the corresponding electrode is defined as a sacrificial zone (SacZ). The two SacZs serve the purpose of dissipating any boundary phenomena that occur at the edges of the SC, such as flow perturbation and bubble generation. In our case, each SacZ area is 10% of the total SC area.

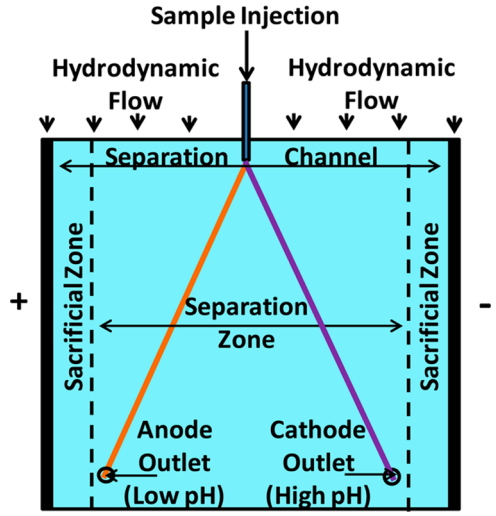

Figure 1. Conceptual illustration of a mFFE device. A sample mixture is carried by a uniform hydrodynamic flow and is electrophoretically separated into a negatively charged analyte stream (orange) and a positively charged analyte stream (purple). In the case of maximum sample separation, the streams are directed toward the terminal collection outlets, anode outlet (AO) and cathode outlet (CO), which define the boundaries between the separation zone (SZ) and the sacrificial zones (SacZ). The SZ area is allocated for unperturbed sample separation while the SacZ areas serve to dissipate the effects of boundary phenomena (i.e., flow perturbation). The difference between buffer pH at AO and CO defines the ΔpH parameter.

H^+ and OH^-, generated at the anode and cathode, respectively, migrate toward the interior of the SC, forming pH and conductivity gradients. The extent to which these gradients permeate the SC depends on the applied electric field strength, buffer concentration, and hydrodynamic flow rate. To avoid any negative effect associated with pH gradients, it is important to ensure that they do not extend into the SZ. The existence of pH gradients in the SacZ areas, however, is inconsequential to mFFE separation efficiency, because the

dx.doi.org/10.1021/ac501081b | Anal. Chem. 2014, 86, 5656−5660

maximum separation distance between two analytes is limited by the distance between the terminal outlets.

By determining the difference in pH at the AO and the CO, we define a parameter, $\Delta pH = pH_{CO} - pH_{AO}$, which reflects the capacity of pH gradients to influence the separation efficiency of the device. Conceptually, a ΔpH equal to 0 indicates a situation in which existing pH gradients do not extend into the SZ. Thus, the goal of pH gradient optimization is to minimize ΔpH.

The minimization of ΔpH can be achieved by increasing the buffer concentration, reducing the electric field strength, or increasing the hydrodynamic flow rate. Typically, the buffer concentration is limited by the highest value at which electrolyte overheating does not occur. In our case, the buffer concentration was limited to 25 mM to prevent boiling of the electrolyte. Both the flow rate and the electric field strength are tuned to obtain desired sample resolution. We were interested to determine the magnitudes of ΔpH when typical mFFE flow rates and electric field strengths are used. mFFE devices have the capacity to reach flow rates as low as 1 mL/min without significant band broadening and electric field strengths of 100 V/cm without overheating. The range of investigated flow rates and electric field strengths were 1−8 mL/min and 25−100 V/cm, respectively. In Figure 2a, it can be observed that a significant increase in ΔpH occurs as flow rates decrease and as electric field strengths increase. Combinations of smaller flow rates with higher electric field strengths further increase ΔpH.

It is important to recognize that the conditions which cause the highest ΔpH values (low flow rates and high electric field strengths) also represent conditions that maximize the electrophoretic separation. pH gradients that permeate the SZ, thus, prevent mFFE from reaching its full potential in terms of separation efficiency. It is desirable, therefore, to minimize ΔpH, while allowing the usage of separation conditions that are most advantageous. This problem can be addressed by implementing modifications to the mFFE device geometry, in particular the geometry of the SacZ areas.

Increasing the depth of the SacZ areas can increase the flow rate within them, without increasing the flow rate in SZ. Deep channels were originally implemented to rapidly remove electrolytic bubbles.[20] The same logic can be applied to remove electrolytic ions. It is possible to calculate the migration time of H^+ and OH^- across the SacZ, since this time is proportional to their electrophoretic mobility. We can make the assumption that the conductivity in the SacZ areas will increase due to the influx of H^+ and OH^- and that this will have a negative effect on both electric field strength and the electrophoretic velocity. Therefore, the minimum migration time will be proportional to the voltage supplied by the power supply. From this information, it is possible to determine the necessary linear flow velocity to evacuate H^+ and OH^- before their migration into the SZ area.

In our mFFE device, we use H^+ as the model since it has the highest electrophoretic mobility (3.6×10^{-7} $m^2/(V{\cdot}s)$).[30] With this knowledge, it was determined that H^+ ions would have to be evacuated from the SacZ within 3 s, in the presence of an 100 V/cm electric field, before migrating into the SZ (see the Supporting Information for calculation). For H^+ ions to be evacuated in less than 3 s, the linear flow velocity within the SacZ would have to be at least 3.3×10^{-2} m/s. This can be achieved, with a buffer flow rate of 1 mL/min, if the depth of the SacZ is increased to 2.4 mm, or 12 times the depth of the SZ. High flow rates in the SacZ areas, however, can affect flow uniformity. In an effort to investigate any influence that deep SacZ areas might have on the hydrodynamic flow profiles in the SZ, we modeled the flow streamlines in a virtual device using COMSOL. It was found that the flow within the SZ does deviate toward the SacZ areas (Figure S2, Supporting Information). We have previously defined a quantitative parameter that described flow uniformity in a FFE device.[22] Flow uniformity is characterized by the ratio of w/w_{tot}, where w is the width of the SZ entry gate which incorporates streamlines of flow that do not enter the SacZ and w_{tot} is the total width of the SZ. Ideally, a w/w_{tot} should be equal to 1. It is important to note that the current definition of w_{tot} is different than what was reported in our previous publication. Formerly, w_{tot} incorporated the entire SC. However, since the SacZs are not used in separation, they should be excluded from w_{tot}. Therefore, from this point forward, all w_{tot} values will only include the SZ. In our virtual mFFE device, we calculated the w/w_{tot} to be 0.62 (Figure S2, Supporting Information). We have previously developed a strategy to alleviate such flow nonuniformity using sacrificial channels.

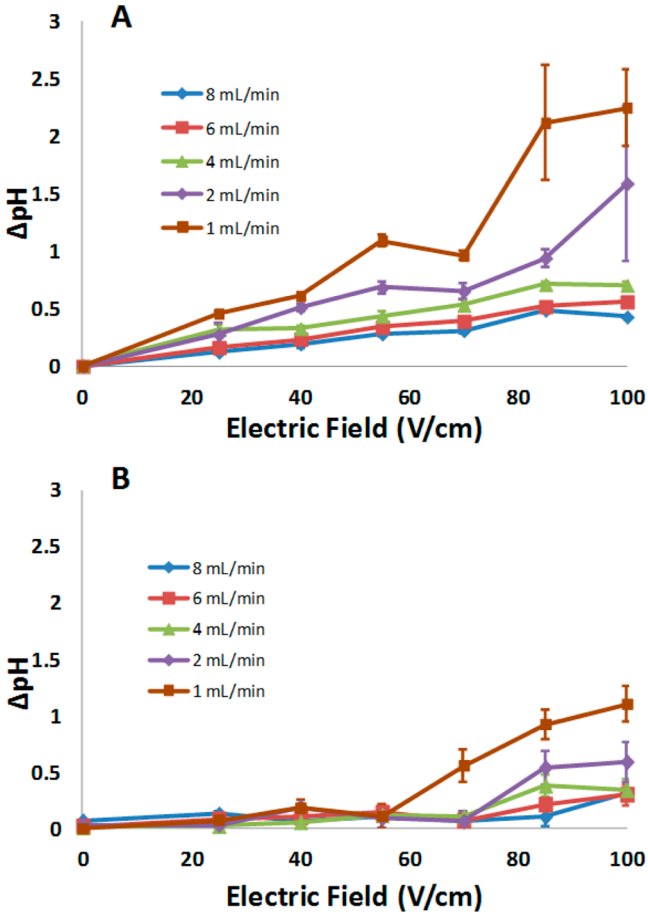

Figure 2. ΔpH between the anode outlet and cathode outlet of a mFFE device without (a) and with (b) sacrificial channels. H^+ and OH^- migrate across the separation channel and change the pH, thus affecting the separation conditions. Naturally, this effect worsens at higher electric field strengths and lower flow rates. Sacrificial channels, integrated in the SacZ areas, provide a region of faster flow that can evacuate H^+ and OH^- more efficiently and limit the change in ΔpH. mFFE devices with sacrificial channels can decrease ΔpH further than devices without sacrificial channels and maintain a uniform pH over a broader range of separation conditions. Error bars represent the standard deviation of three separate pH measurements at each outlet.

dx.doi.org/10.1021/ac501081b | Anal. Chem. 2014, 86, 5656−5660

Sacrificial channels are geometric features that can increase flow uniformity in mFFE devices. These features consist of a series of deep and shallow channels with alternating fast and slow flow rates, where inertial forces dominate within the deep channels and shear forces dominate within the shallow channels. The interplay between these two forces prevents the fluid from diverging from its original trajectories. We have already demonstrated that sacrificial channels can reduce flow nonuniformity in a similar mFFE device.[22] In our new device prototype, we tried to maximize the number of sacrificial channels to attain the best possible reduction in pH gradients and increase of flow uniformity. The specifications of a milling machine, used for device fabrication, limited us to a maximum of 4 sacrificial channels within the SZ. In the device setup highlighted in Figure 1, we optimized the sacrificial channel depth (3.5 mm) to evacuate the ions in a similar time frame as when a single deep channel was used. The integration of 4 sacrificial channels resulted in an increase of w/w_{tot} to 0.86 (Figure S2, Supporting Information). It should be noted that the integration of sacrificial channels does not change the distance between the terminal outlets and, thus, does not reduce the maximum resolving power of the device. In a previous study, we determined that similar sacrificial channels did not influence the quality of separation, and we do not expect the separation to be adversely affected here (Figure S3, Supporting Information).

We have demonstrated the effectiveness of the modified design by implementing it into a real mFFE prototype. The device was fabricated as described elsewhere, and experiments, similar to those described in Figure 2a, were performed. We observed significant decreases in ΔpH over the entire range of conditions (Figure 2b), which implies that the developed solution was effective in minimizing pH gradients across the SZ. In fact, negligible changes in ΔpH were observed when all flow rates were applied up to an electric field strength of 55 V/cm. The same improvement was observed for 70 V/cm at all flow rates except 1 mL/min. Bubbles did not pose a problem to the stability of the electric field because they were evacuated rapidly by high flow rates within the sacrificial channels. Furthermore, we observed that the electric current was not affected by the presence of sacrificial channels in the SacZ. This suggests that the proposed solution reduces ΔpH, over a wider range of experimental conditions, and does so without compromising the electric field strength, unlike ion-exchange membranes. These findings allow us to use mFFE at its full potential.

CONCLUSION

For the first time, we demonstrate that electrolytic ions contribute to the formation of significant pH gradients in mFFE. To reduce these pH gradients, we have developed an optimization strategy in which mFFE device geometry was modified. We hypothesized that increasing the flow rate in the SacZ areas would evacuate the ions and they would be unable to enter into the SZ, thereby, mitigating pH gradients. In an optimized mFFE prototype, we integrated deep and wide SacZ areas and observed that pH gradients were minimized, even at low flow rates and high electric field strengths. mFFE can now be used over a broader range of experimental conditions, making this technique a more feasible complement to small-volume CFS.

ASSOCIATED CONTENT

Supporting Information

Additional information as noted in text. This material is available free of charge via the Internet at http://pubs.acs.org/.

AUTHOR INFORMATION

Corresponding Author

*E-mail: skrylov@yorku.ca.

Notes

The authors declare no competing financial interest.

ACKNOWLEDGMENTS

Funding for this research was generously provided by NSERC Canada.

REFERENCES

(1) Yoshida, J.-I.; Takahashi, Y.; Nagaki, A. *Chem. Commun.* **2013**, *49*, 9896−9904.
(2) Song, H.; Tice, J. D.; Ismagilov, R. F. *Angew. Chem., Int. Ed.* **2003**, *42*, 768−772.
(3) Jovanovic, J.; Rebrov, E. V.; Nijhuis, T. A.; Hessel, V.; Schouten, J. C. *Ind. Eng. Chem. Res.* **2010**, *49*, 2681−2687.
(4) Sauks, J. M.; Mallik, D.; Lawryshyn, Y.; Bender, T. P.; Organ, M. G. *Org. Process Res. Dev.* **2013**, ASAP Article.
(5) Wiles, C.; Watts, P.; Haswell, S. J.; Pombo-Villar, E. *Tetrahedron* **2005**, *61*, 10757−10773.
(6) Ullah, F.; Samarakoon, T.; Rolfe, A.; Kurtz, R. D.; Hanson, P. R.; Organ, M. G. *Chem.−Eur. J.* **2010**, *16*, 10959−10962.
(7) Mastronardi, F.; Gutmann, B.; Kappe, C. O. *Org. Lett.* **2013**, *15*, 5590−5593.
(8) Moore, J. S.; Jensen, K. F. *Org. Process Res. Dev.* **2012**, *16*, 1409−1415.
(9) Malet-Sanz, L.; Susanne, F. *J. Med. Chem.* **2012**, *55*, 4062−4098.
(10) McMullen, J. P.; Jensen, K. F. *Annu. Rev. Anal. Chem.* **2010**, *3*, 19−42.
(11) Reichart, B.; Tekautz, G.; Kappe, C. O. *Org. Process Res. Dev.* **2013**, *17*, 152−157.
(12) Roth, G. P.; Stalder, R.; Long, T. R.; Sauer, D. R.; Djuric, S. W. *J. Flow Chem.* **2013**, *3*, 34−40.
(13) Carroccia, L.; Musio, B.; Degennaro, L.; Romanazzi, G.; Luisi, R. *J. Flow Chem.* **2013**, *3*, 29−33.
(14) Wiles, C.; Watts, P. *Eur. J. Org. Chem.* **2008**, 1655−1671.
(15) deMello, A. J. *Nature* **2006**, *442*, 394−402.
(16) Hannig, K.; Wirth, H.; Meyer, B.-H.; Zeiller, K. *Hoppe-Seyler's Z. Physiol. Chem.* **1975**, 1209−1223.
(17) Hannig, K.; Wirth, H.; Schindler, R. K.; Spiegel, K. *Hoppe-Seyler's Z. Physiol. Chem.* **1977**, *358*, 753−764.
(18) Kohlheyer, D.; Eijkel, J. C. T.; Schlautmann, S.; van den Berg, A.; Schasfoort, R. B. M. *Anal. Chem.* **2008**, *80*, 4111−4118.
(19) Kohler, S.; Weilbeer, C.; Howitz, S.; Becker, H.; Beushausen, V.; Belder, D. *Lab Chip* **2011**, *11*, 309−314.
(20) Fonslow, B. R.; Barocas, V. H.; Bowser, M. T. *Anal. Chem.* **2006**, *78*, 5369−5374.
(21) Eigeldinger, J.; Vogt, H. *Electrochim. Acta* **2000**, *45*, 4449−4456.
(22) Agostino, F. J.; Cherney, L. T.; Galievsky, V.; Krylov, S. N. *Angew. Chem., Int. Ed.* **2013**, *52*, 7256−7260.
(23) Millioni, R.; Franchin, C.; Tessari, P.; Polati, R.; Cecconi, D.; Arrigoni, G. *J. Chromatogr., A* **2013**, *1293*, 1−9.
(24) Heydt, A.; Mosher, R. A. *Electrophoresis* **1989**, *10*, 697−704.
(25) Kohlheyer, D.; Besselink, G. A. J.; Schlautmann, S.; Schasfoort, R. B. M. *Lab Chip* **2006**, *6*, 374−380.
(26) Turgeon, R.; Bowser, M. T. *Anal. Bioanal. Chem.* **2009**, *394*, 187−198.
(27) Yin, X.-Y.; Dong, J.-Y.; Wang, H.-Y.; Li, S.; Fan, L.-Y.; Cao, C.-X. *Electrophoresis* **2013**, *34*, 2185−2192.
(28) Jezierski, S.; Belder, D.; Nagl, S. *Chem. Commun. (Cambridge, U. K.)* **2013**, *49*, 904−906.

(29) Agostino, F. J.; Evenhuis, C. J.; Krylov, S. N. *J. Sep. Sci.* **2011**, *34*, 556−564.
(30) Duso, A. B.; Chen, D. D. *Anal. Chem.* **2002**, *74*, 2938−2942.

ELECTRONIC SUPPLEMENTARY INFORMATION

Reducing pH Gradients in Free-Flow Electrophoresis

Fletcher J. Agostino, Leonid T. Cherney, Mirzo Kanoatov, and Sergey N. Krylov*

Chemistry Deparment and the Centre for Research on Biomolecular Interactions,

York University, Toronto, Canada

Chip Fabrication

All sszFFE prototypes were fabricated from poly(-methyl methacrylate) stock material using a MDX-540 robotic milling machine. The optimized cutting speeds for the end mills have already been described in full detail, including assembly of prototypes (*J. Sep. Sci*., 2011, 34, 556-564). Briefly, the fabrication of sszFFE involves milling the bottom, and top substrates. The three substrates are then bonded together using small volumes of dichloromethane (CH_2Cl_2). CH_2Cl_2 was injected carefully to provide a tight seal at the edges of the device. The device was clamped together for 10 min to allow the solvent to completely perfuse and dry at the edges. The separation channel is 80 mm long, 100 mm wide, and 0.2 mm deep. Platinum electrodes (80 mm long and 0.75 mm in diameter) were installed into deep electrode channels (1.5 mm deep) and connected with insulated copper wires to a power source (**Fig. S1b**). Additional milling of narrow and deep channels (3.5 mm deep and 1.5 mm wide) was performed for sszFFE prototypes with integrated sacrificial channels (**Fig. S2c**).

Chip Schematic

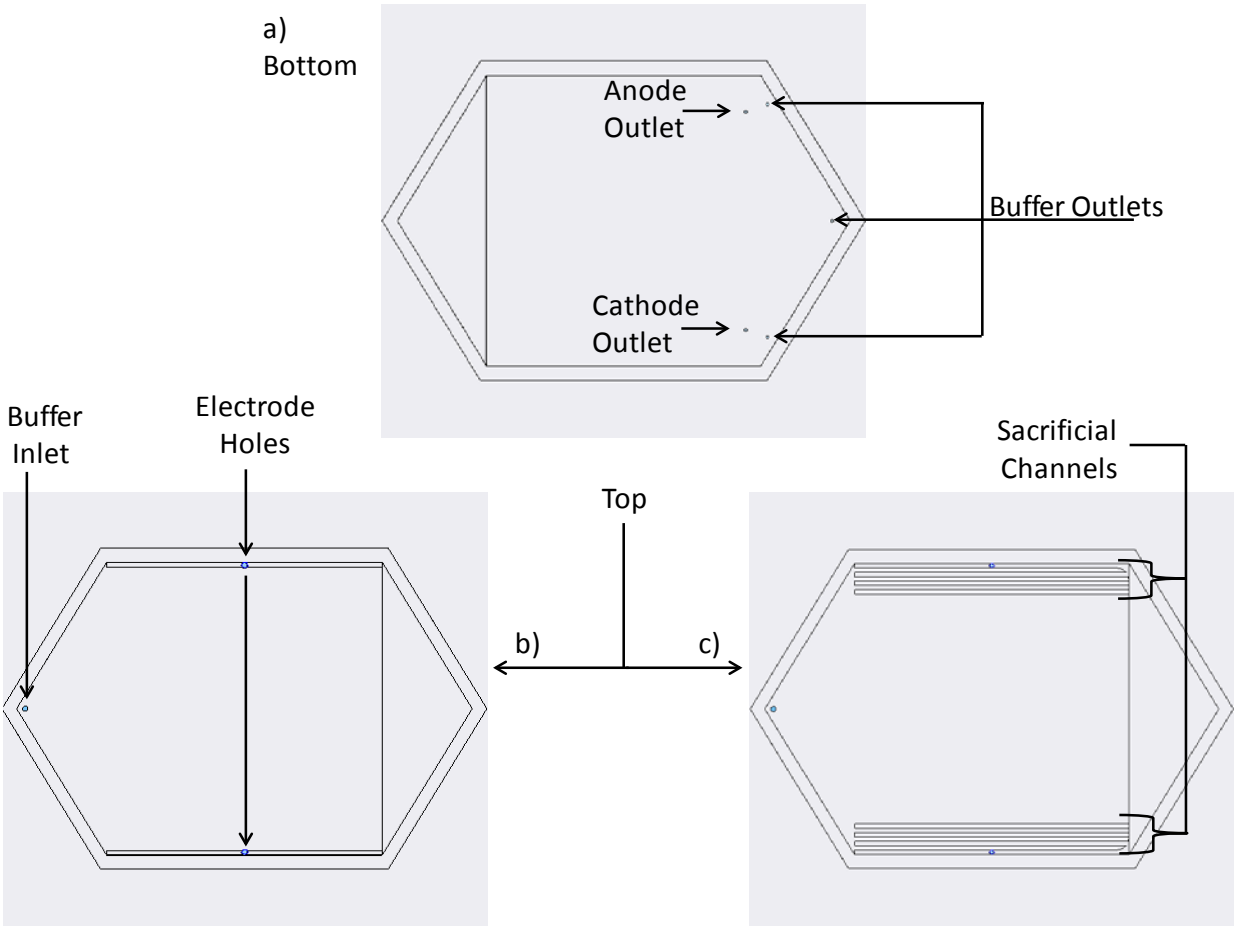

Figure S1: Schematic of mFFE bottom (a) and top (b and c) substrates using Solid Edge CAD software. Here, the outputs for the buffer, and anode and cathode outlets are shown. In (b) and (c) the buffer is introduced in the top substrate. The electrode wires protrude from the mFFE device, through the electrode holes, to facilitate contact with the copper wire. The sacrificial channels in (c) represent the deep geometric features that increase the flow rate to evacuate H^+ and OH^- before creating a significant pH gradient across the width of the separation channel.

Electrode Reactions and Volume Reactions Involving H^+ and OH^-

$$\mathrm{B^- + H^+ \underset{k_b}{\overset{k_{ah}}{\rightleftharpoons}} BH}, \qquad K_b = \frac{k_b}{k_{ah}}$$

$$\mathrm{BH + OH^- \underset{k_a}{\overset{k_{bd}}{\rightleftharpoons}} H_2O + B^-}, \quad K_a = \frac{k_a}{k_{bd}} \qquad (1)$$

$$\mathrm{H^+ + OH^- \underset{k_w}{\overset{k_{hd}}{\rightleftharpoons}} H_2O}, \qquad K_w = \frac{k_w}{k_{hd}}$$

$$R_i = \nabla \cdot (-D_i \nabla c_i - z_i u_{m,i} F c_i \nabla V) + v \cdot \nabla c_i \qquad (2)$$

where R_i, for each species, is:

$$\begin{aligned}
R_b &= k_{ah}(c_a c_h - K_b c_b) - k_{bd}(c_b c_d - K_a c_a) \\
R_a &= -k_{ah}(c_a c_h - K_b c_b) + k_{bd}(c_b c_d - K_a c_a) \\
R_h &= -k_{ah}(c_a c_h - K_b c_b) - k_{hd}(c_h c_d - K_w) \\
R_d &= -k_{bd}(c_b c_d - K_a c_a) - k_{hd}(c_h c_d - K_w)
\end{aligned} \qquad (3)$$

COMSOL Theory and Equations

To simulate mFFE devices we used COMSOL. The steady state Navier-Stokes equation was used for the *in-silico* computations, with the condition of non-compressible flow. The laminar flow physics model was chosen and we input a flow into the electrolyte inlet (**Fig. S1a)**. The boundary conditions include: no-slip walls; laminar inflow at the inlet; and no viscous stress at the outlet. The meshing geometry used was tetrahedral, with a fine size in areas of large volume (exit and entrance reservoirs, and SacZ area), and extremely fine geometry in the SZ area. Default stabilization conditions (with a tuning parameter $C_k = 1$) were selected: streamline diffusion and crosswind diffusion. 3-D models were prepared to fully capture the flow system in only one half of the device to reduce simulation time. The mathematical model includes the following relations.

Laminar flow equations inside the device:

$$\rho(v \bullet \nabla)v = \nabla \bullet \left\{ -pI + \mu\left[\nabla v + (\nabla v)^T\right] \right\} \qquad (1)$$

$$\rho \nabla \bullet v = 0 \qquad (2)$$

Wall boundary condition:

$$v = 0 \qquad (3)$$

Inlet condition:

$$L_{\text{entr}}\nabla_t \bullet\left\{-p_{\text{enter}}I+\mu\left[\nabla_t v+\left(\nabla_t v\right)^T\right]\right\}=-p_{\text{enter}}n \tag{4}$$

$$\nabla_t \bullet v=0 \tag{5}$$

Outlet condition:

$$p=p_0,\quad \left[\mu\left(\nabla v+\left(\nabla v\right)^T\right)\right]\bullet n=0 \tag{6}$$

Symmetry conditions at the symmetry plane $x = 0$:

$$v\bullet n=0,\quad K-\left(K\bullet n\right)n=0 \tag{7}$$

$$K=\left[\mu\left(\nabla v+\left(\nabla v\right)^T\right)\right]n \tag{8}$$

where, ρ and μ are density and viscosity of the liquid; v and p are the velocity and pressure; K is the viscous force at the symmetry plane; p_{enter} and p_0 are the pressures at the inlet and outlet, respectively; L_{entr} is a parameter used by COMSOL in the inlet condition; I is the unit tensor; n is the normal to the walls or to the symmetry plane; the superscript T denotes a transpose matrix.

Hydrodynamic Flow Trajectory within SacZ areas

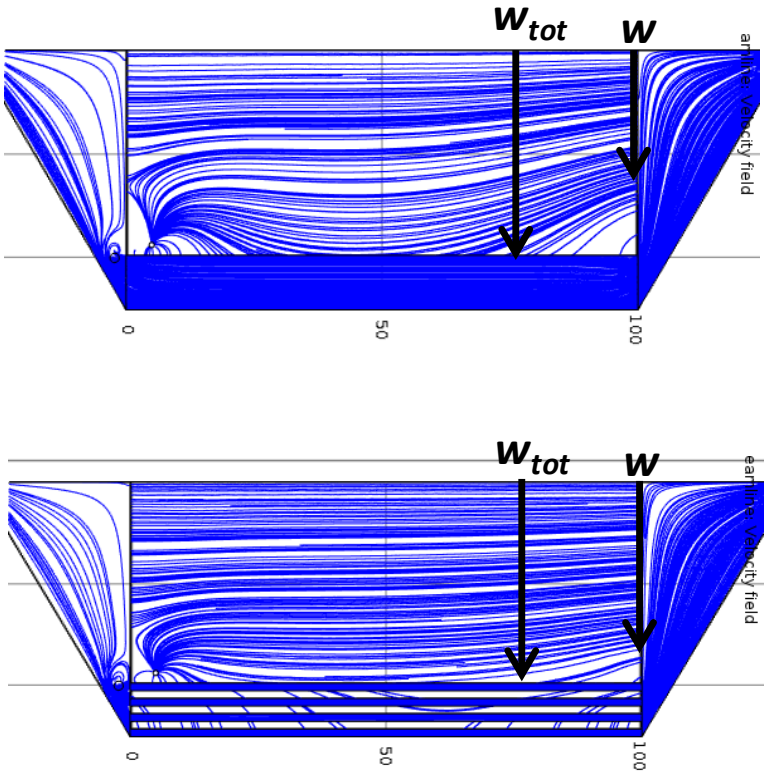

$w/w_{tot} = 0.62$

$w/w_{tot} = 0.86$

Figure S2: COMSOL simulation of buffer flow showing the top-view of a mFFE device. Only one half of the virtual model is illustrated. In both devices, the flow is 8 mL/min. In the top panel the depth of the SacZ area is 2.4 mm, this causes flow-non uniformity to exist in the SZ. Flow uniformity is characterized by the ratio of w/w_{tot}, where w is the width of the SZ entry gate which incorporates streamlines of flow that do not enter the SacZ and w_{tot} is the total width of the SZ. Ideally, a w/w_{tot} should be equal to 1. In the top panel the resultant w/w_{tot} = 0.62. In the bottom panel, sacrificial channels are introduced. The depth of the deep channels is 3.5 mm in order to remove electrolytic ions before their migration into the SZ, but the shallow channels remain 0.2 mm deep. Flow uniformity is improved which is indicated by the increased value of the w/w_{tot} = 0.86.

Calculating the maximum electrophoretic velocity of H^+ at 100 V/cm, and the necessary velocity within SacZ to evacuate H^+

Electrophoretic mobility of H^+: 3.6×10^{-7} $m^2/(Vs)$

Electric field strength: 10^4 V/m

Therefore the electrophoretic velocity of H^+: $\left(3.6\times10^{-7}\ \frac{\text{m}^2}{\text{Vs}}\right)\left(10^4\ \frac{\text{V}}{\text{m}}\right) = 3.6\times10^{-3}\ \frac{\text{m}}{\text{s}}$

Width of the Sacrificial Zone (SZ): 0.001 m

Time for H^+ to travel across the SZ width: $\frac{0.010\ \text{m}}{3.6\times10^{-3}\ \frac{\text{m}}{\text{s}}} \approx 3\,\text{s}$

Therefore, the flow within the SZ needs to be fast enough to evacuate H^+ in less than 3 s.

Length of SZ: 0.08 m

Flow velocity necessary within SZ: $\frac{0.10\ \text{m}}{3.0\ \text{s}} = 0.033\,\frac{\text{m}}{\text{s}}$

Hagen-Poisuelle equation was re-arranged to approximate the channel height necessary to provide the required velocity of 0.033 m/s

$$H = \sqrt{\frac{12v\eta L}{\Delta P}} = \sqrt{\frac{12(0.033)(0.001)(0.08)}{5.5}} = 0.0024\text{m}$$

Where v is the fluid velocity, L is the length of the channel, P is the pressure, and η is electrolyte viscosity. ΔP is calculated from COMSOL as the pressure difference from the entry and exit of the SC.

Separation of Two Dyes in the Presence of Sacrificial Channels

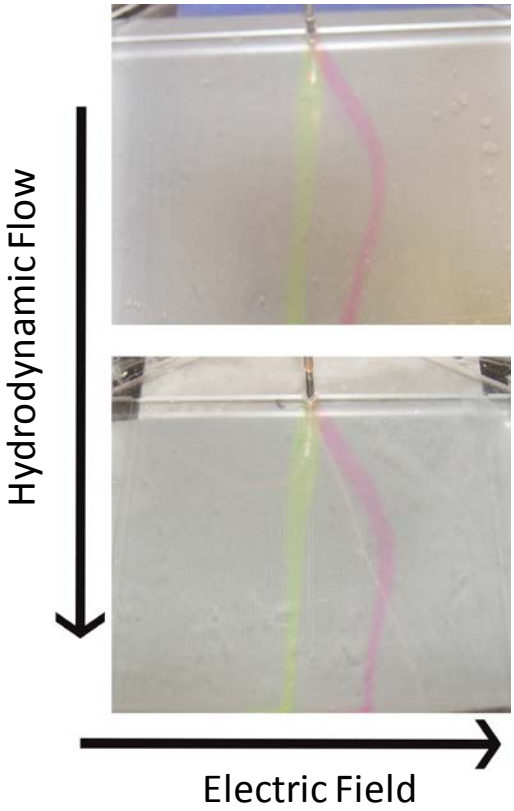

Figure S3: The separation of fluorescein and rhodamine B in a mFFE-scale device. Here, the two dyes are separated using a device without sacrificial channels (top) and with sacrificial channels (bottom). We demonstrated that the presence of sacrificial channels has no negative influence on separation quality. The hydrodynamic flow rate is 8 mL/min and the sample flow rate is 5 µL/min, and the electric field strength is 50 V/cm.